Available online at www.sciencedirect.com
SCIENCE DIRECT
Journal of the European Ceramic Society 26 (2006) 1715–1724
www.elsevier.com/locate/jeurceramsoc

New porous silicon carbide composite reinforced by intact high-strength carbon fibres

Juliane Mentz [a,*], Marcus Müller [a], Meinhard Kuntz [b], Georg Grathwohl [b], Hans Peter Buchkremer [a], Detlev Stöver [a]

[a] *Institut für Werkstoffe und Verfahren der Energietechnik (IWV-1), Forschungszentrum Jülich GmbH, D-52425 Jülich, Germany*
[b] *Keramische Werkstoffe und Bauteile, Fachbereich Produktionstechnik, Universität Bremen, IW3, Am Biologischen Garten 2, D-28359 Bremen, Germany*

Received 12 January 2005; received in revised form 14 March 2005; accepted 19 March 2005
Available online 10 May 2005

Abstract

A novel processing method to produce a carbon-fibre-reinforced silicon carbide (C/SiC) is presented and the mechanical properties are evaluated. The low-cost process yields a reaction bonded silicon carbide matrix but avoids efficiently reactive damage of the carbon fibres. Thus, the C/SiC-material shows a fibre-dominated behaviour due to high fibre strength and matrix porosity. The characteristics and mechanical properties of this C/SiC are highlighted. The discussion deals with the particular mechanical characteristics of porous-matrix materials relating to similar materials investigated hitherto.

Keywords: Composites; Porosity; Fracture; Mechanical properties; Toughness; SiC; C/SiC

1. Introduction

In the field of high temperature applications, the use of ceramics is promising due to their constant strength up to high temperatures and their corrosion resistance. However, their brittle damage behaviour impedes their broad industrial use. The implementation of fibre technology overcomes the poor damage tolerance of ceramic materials by a fibre reinforcement (ceramic matrix composites—CMCs).[1–3] Due to the high thermal stability of carbon, research on carbon-fibre-reinforced carbon has been conducted for aerospace applications since the 1970s. In order to avoid this material's poor resistance to oxidising atmosphere at higher temperatures, further development to carbon-fibre-reinforced silicon carbide (C/SiC) followed.

The properties of ceramic matrix composites are determined not only by the fibres and matrix themselves, but also mainly by the microstructure of the matrix and the properties of the fibre-matrix-interface.[4–6] Thus, the manufacturing method has a great influence on the composite properties. In the case of C/SiC there are broadly three processing routes with several modifications reported.[1,7–10] Chemical vapour infiltration (CVI)[11–14] as well as liquid polymer infiltration (LPI)[15–18] exhibit relatively high processing costs. Both methods lead to high-performance materials with stiff matrices. As described by He and Hutchinson,[19] a low fibre-matrix-adhesion is needed in this case to achieve a crack deflecting interface and therefore the desired damage tolerance. Thus, fibre coatings such as carbon or boron nitride are necessary, which not only further increase the processing costs and complexity, but also frequently exhibit a low stability in oxidising environments.[7]

Liquid silicon infiltration (LSI) is a method, which leads to a material with quite different properties. A porous carbon-fibre-reinforced carbon is formed by pyrolysis of a C-rich resin matrix and subsequently infiltrated with molten silicon (melting point approximately 1420 °C). Silicon carbide

* Corresponding author.
E-mail address: j.mentz@fz-juelich.de (J. Mentz).

0955-2219/$ – see front matter © 2005 Elsevier Ltd. All rights reserved.
doi:10.1016/j.jeurceramsoc.2005.03.250

is formed instantaneously. In comparison to CVI and LPI, the LSI process is a relatively low-cost method.[8,20–22] However, the reaction of liquid silicon with solid carbon is not restricted to the carbon of the matrix. It reacts also with the carbon fibres. A homogeneous infiltration with silicon and thus a high content of silicon carbide results in low strength and brittle behaviour of the composite. In the case of low silicon-uptake, the carbon fibres are to a large extent surrounded by carbon material and are therefore available for strengthening. The resulting material is composed inhomogeneously of carbon-fibre-reinforced carbon (C/C) surrounded by silicon carbide and residual free silicon.[23] These materials have been described widely being called C/C-SiC due to the high content of carbon within the matrix.

In the scope of this work a novel processing route was developed to overcome the main disadvantage of the liquid silicon infiltration (LSI) technique – the fibre attack, while retaining the cost efficiency. In the novel route, fine silicon powder is added to the polymer precursor. Thus, before silicon-carbon reaction silicon and carbon are distributed homogeneously within the matrix and the reaction is therefore restricted mainly to the matrix.

This method is called "in-situ silicon–carbon reaction" and leads to a highly porous matrix material. In this case, the stiffness of the matrix is significantly lower than that of the carbon fibres. The elastic mismatch is high. According to the analysis of He and Hutchinson,[19] fibre-matrix-debonding (i.e. crack deflecting interface) is therefore possible even in the case of a strong fibre-matrix-adhesion. Cost intensive fibre coatings are thus not necessary. The mechanical properties of these materials are determined by the fibres and the material is therefore characterised as "fibre-dominated".[24–26] It is assumed that matrices with a low stiffness do not take over axial forces from the fibres to a substantial extent. Consequently, stress redistribution between fibres is limited, and so the strength and fracture toughness are lower than those of composites with stiff matrices. Inherent to the system is also a low strength perpendicular to fibre axis as well as a low interlaminar shear strength.

Even though one of the earliest ceramic matrix composites – carbon-fibre-reinforced carbon (C/C) – is among these fibre-dominated materials, the mechanical properties of porous matrix composites did not enter the literature until the mid 1990s.[27,28] They have as yet been investigated mainly for materials with oxide fibres and oxide matrix (oxide/oxide composites).[3,24–31] It is concluded that the function of the highly porous matrix material is to isolate fibres from cracks within the matrix.[3,29] The fracture behaviour is referred to the damage effects of the matrix material and the consequence for neighbouring fibres. Due to the highly porous matrix material, energy is dissipated and stress concentrations around a fibre fracture or a matrix crack is low. Crack propagation to the neighbouring fibres is inhibited[32] and the fibres stay intact according to their statistical fracture stress distribution like a fibre bundle. The fracture surfaces of fibre-dominated materials show in the ideal case a similar fibre pullout with brush-like fracture surface as the more conventional materials with dense matrices, albeit there is almost no matrix material left. Some residues of matrix material adhere to the fibres.[29]

To achieve a high strength perpendicular to the fibre axis, the matrix porosity should nevertheless be as small as is possible consistent with a tolerant failure behaviour. Studies of the influence of further reinfiltration steps to reduce the matrix porosity[33,34] show that several effects such as inhomogeneities, fibre distribution and especially size, form and distribution of the pores influence the sustainment of initial-debonding. Inhomogeneities result in dense regions with a brittle damage behaviour. A crack starting in such a region continues straight through the whole cross-section due to a high energy release and causes premature failure of the component.

This paper deals with the mechanical properties of fibre-dominated materials with porous matrices in non-oxide composites. First, the developed processing method in-situ silicon-carbon reaction for C/SiC with a porous matrix is described. The configuration and microstructure of the resulting material as well as modifications of composition and reinforcement are described in section two permitting a detailed discussion of the mechanical results. The third section describes the mechanical testing methods. The results of mechanical testing are presented and discussed in Section 4. Conclusions are given in Section 5.

2. Processing and microstructure

In the developed processing method, in-situ silicon-carbon reaction, a matrix suspension consisting of silicon powder (Si-M.P. AX20, H.C. Starck, Germany) in phenolic resin (K790, Bakelite AG, Germany) dissolved in isopropanol is prepared first. The average particle size of silicon was reduced by milling to a value significantly lower than the diameter of the carbon fibres ($d = 7\ \mu m$) in order to obtain a close packing of silicon particles around the fibres. The fibre bundle (HTA 5131, Tenax Fibers GmbH & Co. KG, Germany) is impregnated with the suspension as shown in Fig. 1. A winding machine is used to produce unidirectional reinforced prepregs. After drying, the prepregs are cut and stacked in a mould. Curing of the resin is performed in a heatable press at a maximum temperature of 190 °C under a pressure of 20 MPa. A component of carbon-fibre-reinforced plastic (CFRP) is formed.

During carbonisation up to 950 °C in argon atmosphere, the phenolic resin is transformed into glassy carbon. This is accompanied by a weight loss of 45% (i.e. volume reduction 54%). Thus, due to a low shrinkage of the composite (approx. 5%) the porosity increases up to a value of 15–20%. After carbonisation the matrix consists of silicon and carbon in stochiometric ratio homogeneously distributed within the matrix. In the final thermal treatment step – the silicon-carbon reaction – the reaction of liquid silicon and solid carbon to form silicon carbide within the matrix is carried out

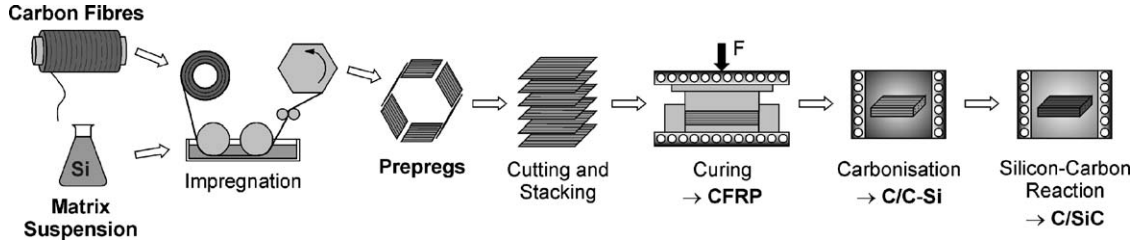

Fig. 1. Schematic of processing method for carbon-fibre-reinforced silicon carbide with porous matrix.

at a temperature slightly above the melting point of silicon (1450 °C, vacuum). Silicon carbide is of higher density than silicon and carbon, but the shrinkage of the composite due to the reaction is again hindered by the fibre reinforcement. This leads to a further increase of the composite's porosity to a value of more than 30% with a corresponding low total density of approximately 1.5 g/cm^3. The final product of carbon-fibre-reinforced silicon carbide (C/SiC) is achieved.

2.1. Unidirectional reinforced C/SiC

XRD-measurements confirm the formation of silicon carbide (Fig. 2). There is no free silicon left after the silicon-carbon reaction. The broad carbon-peak is associated to the carbon fibres. Free carbon within the matrix was not detectable by this method due to its amorphous structure. Thus, a minor excess of carbon within the matrix is possible.

In Fig. 3 the pore size distribution of the material – measured via mercury intrusion – is shown. The material contains a small amount of large pores and cracks between 10 and 100 μm, which do not change during the silicon-carbon reaction. Larger voids could not be detected.

During carbonisation the phenolic resin is transformed into glassy carbon. This is accompanied by a shrinkage and a generation of porosity. Investigations using silicon with an intentionally larger particle size made it possible to observe the position of pore formation. Fig. 4 shows such a material after carbonisation. During the transformation of phenolic resin into glassy carbon, the pores are evidently formed around the silicon particles. When silicon of a small particle size is used, these pores are very small with a narrow distribution (pore size of approximately 0.01 μm, Fig. 3). Furthermore, the glassy carbon adheres to the carbon fibres, which indicates a high adhesive strength.

A geometrical calculation indicates a significantly higher total porosity (17%) than the open porosity measured by mercury intrusion (13%, Table 1). The slope of the curve in the range of small pore radii (<0.01 μm, Fig. 3) suggests that saturation is not reached. The characterisation of pore size by BET method revealed a further amount of pores in the range below 2 nm. Thus, measurements of the specific surface by this method showed a high specific surface, almost one order

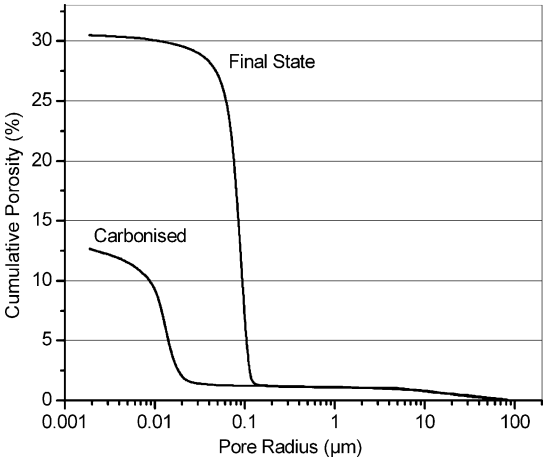

Fig. 3. Pore size distributions of unidirectional reinforced material, carbonised and final state.

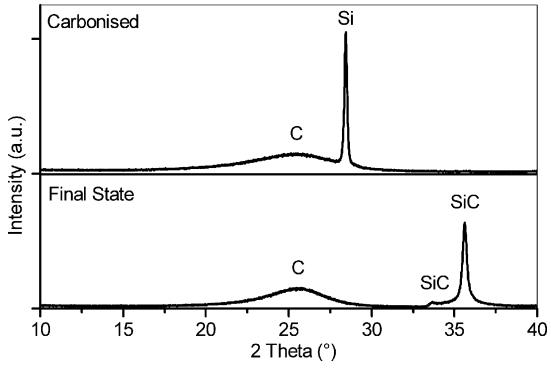

Fig. 2. XRD-measurements of the developed material, carbonised and final state.

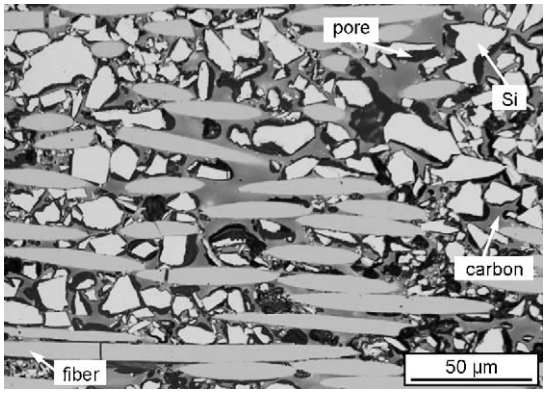

Fig. 4. Optical micrograph of a polished cross section of a carbonised material with silicon of greater particle size.

Table 1
Unidirectional carbon-fiber-reinforced silicon carbide: total porosity and specific surface, comparison of measurement methods

Measurement method	Porosity (%)		Specific surface (m^2/g)	
	Mercury intrusion	Geometrical	Mercury intrusion	BET
Carbonised	13 ± 2	17 ± 1	19 ± 3	98 ± 9
Final state	32 ± 2	33 ± 2	8 ± 4	13 ± 2

of magnitude higher than that calculated from the results of mercury intrusion (98 versus 19 m^2/g, Table 1).

As described above, during the silicon-carbon reaction the total porosity increases up to a value of more than 30%. The porosity measured by mercury intrusion was now almost identical to the geometric porosity, which clearly indicates a totally open porosity (Table 1). The pore radii of the matrix pores also increase during silicon-carbon reaction. Now, there is again a narrowly distributed porosity with a pore size of approximately 0.1 μm. The specific surface calculated from the results of mercury porosimetry was in good agreement with the values measured using the BET method (Table 1).

A cross section of unidirectional reinforced C/SiC produced by the in-situ silicon-carbon reaction perpendicular to fibre axis is shown in Fig. 5. The originally round cross section of the carbon fibres is preserved, no indications of fibre damage are found. In contrast to the liquid silicon infiltration technique, the fibre attack could be minimised since the silicon is well distributed and mixed intimately with the carbon of the matrix. The original matrix materials phenolic resin and silicon powder and therefore the resulting silicon carbide matrix material are distributed homogeneously around the fibres, also in small gaps. Only a few large pores are visible within a fibre bundle. The high matrix porosity can also be seen in the micrograph of Fig. 5.

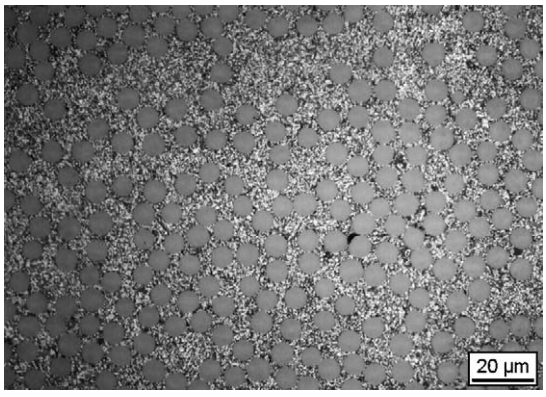

Fig. 5. Optical micrograph of a transverse polished cross section of a unidirectional reinforced C/SiC after silicon-carbon reaction.

2.2. Modifications

2.2.1. Modification of the matrix composition

Besides the "stoichiometric" composition, the effects of an excess of carbon ("C-excess", 30 wt.%) and silicon

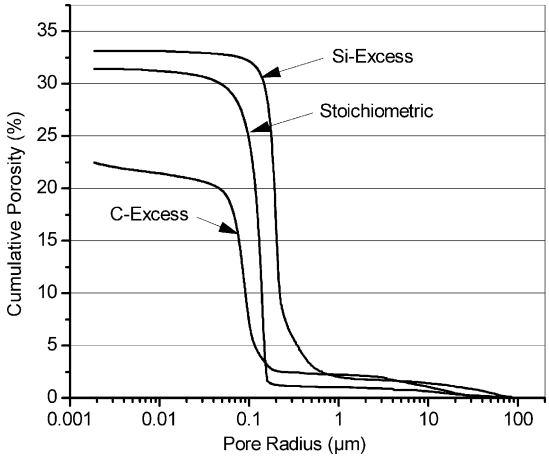

Fig. 6. Pore size distributions of unidirectional reinforced material with different matrix compositions.

("Si-excess", 20 wt.%) within the matrix, respectively were investigated. The differences in the concentration of filler particles (silicon grains) in the resin led to different fibre volume fractions, which has to be considered in the discussion of mechanical properties. On the other hand, a different pore size distribution was detected (Fig. 6). With increasing ratio of silicon within the matrix the total porosity as well as the mean pore size increases. In the case of the matrix composition with silicon excess this is an unexpected result and will be further discussed below. The total porosity of the C/SiC-material is given by the processing route and the matrix composition. With a value of approximately 60% for the stoichiometric matrix material it is relatively high compared to related oxide/oxide-materials[29] (matrix porosity of 35–40%). Limited influences are possible due to the type of resin (modification in shrinkage), for example.

2.2.2. Modification of the direction of reinforcement

In the previous sections a unidirectional fibre reinforcement is described. For comparison, a 0/90°-laminate was also produced in order to investigate the changes in mechanical properties. A micrograph of a polished cross section of such a laminate is shown in Fig. 7, where the different layers can easily be distinguished.

In contrast to the material with unidirectional reinforcement the shrinkage during carbonisation (transformation of resin into glassy carbon) is hindered in two directions (in plane). Thus, segmentation cracks parallel to the fibre axis are formed. These cracks do not change during silicon-carbon reaction and lead to a bimodal pore size distribution and a higher total porosity of the composites (35 ± 2% versus 33 ± 2% for stoichiometric matrix composition). Since the segmentation cracks are caused by the transformation of the resin, they decrease with increasing silicon-content of the matrix (decreasing content of phenolic resin), and thus are largest at C-excess and smallest at Si-excess.

In the ideal case, the matrix material covers each single fibre and is thus able to minimise stress peaks and to optimise

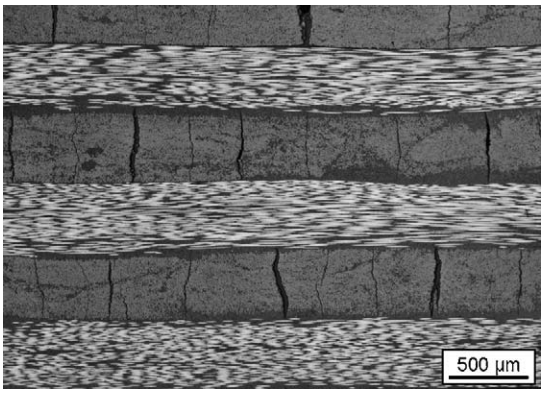

Fig. 7. Optical micrograph of a polished cross section of C/SiC with bidirectional fibre reinforcement.

the desired effects of the porous matrix material. Thus, for bidirectional reinforced material the impregnation of fibre bundles is favourable compared to the impregnation of fabrics. The filler particles (silicon) cannot be distributed homogeneously between the single fibres due to sieving effects if the fibre bundles are strongly interweaved in a fabric.

3. Mechanical characterisation

The dimensions of the specimens for mechanical characterisation were chosen as follows: width 10 mm, thickness of approximately 3 mm (six layers) and length 110 mm. They were cut using a diamond saw blade. The stiffness of the material in the elastic region was measured with a four-point-bending test with bearing distances of 60 and 20 mm using strain gauges. For the purpose of reduced shear stresses, the bending strength and stress-strain-diagrams were determined using a three-point-bending test with a bearing distance of 90 or 100 mm. The bending tests were performed at constant speed using an automated, electro-mechanical universal testing machine (Zwick 1387 of Zwick, Germany) with a crosshead speed of 0.5 mm/min. At least 10 specimens were measured in each case for statistical significance.

High temperature bending tests were performed in an inert gas furnace at temperatures of 1000 and 1500 °C. The bearings consisted in this case of C/C-material and were heated together with the specimens. For comparison, some specimens were also tested at room temperature (24 °C) in this testing equipment. At each temperature, at least five specimens were tested.

The Zwick testing machine was also used to determine the shear strength. In this case, a three-point-bending configuration was used with a short bearing distance of 25 mm. Again at least 10 specimens of each material modification were tested. Also, shorter bearing distances[35] (15 mm) were tried but these caused squeezing of the specimens leading to too high apparent shear strength values. The values of stiffness, strength and strain for all measurements were derived from linear bending theory.

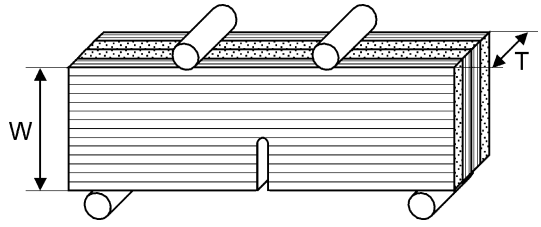

Fig. 8. Scheme of four-point-configuration for SENB-test.

Failure of CMCs is a process of crack propagation and crack branching, crack bridging of the fibres, and finally fibre failure in the crack wake. In order to utilise the strength of the individual fibres and to obtain a damage tolerant fracture behaviour it is necessary that fibre-debonding and therefore an uncorrelated fibre fracture take place. These features are examined advantageously in experiments with stable crack extension. This was realised with single edge notch beam-tests (SENB). Again, this is a four-point-bending test with bearing distances of 60 and 20 mm. In this case, specimens with a thickness of approx. 5 mm (12 layers) were used, with a starting notch (width of 0.5 mm) having a length of one third up to one half of the specimen width produced using a diamond saw blade. In the test, the specimens were oriented edgewise so that a crack spread out in the direction of the starting notch (Fig. 8). This test could not be applied to the unidirectional fibre composites due to delamination. Thus, 0/90°-laminates (eight specimens in each case) with different matrix compositions were tested.

The crack grew in the direction of the starting notch and therefore the bridging of the crack by the fibres was the dominant factor and the effect of reinforcement could be investigated. The load-displacement-curves and fracture surfaces were analysed according to Rausch et al.[36] and Kuntz[37] to evaluate the fracture toughness and failure behaviour. The load is normalised in terms of the formal stress intensity factor $K_{\mathrm{I,form}} = \sigma\sqrt{a_0}Y$ where a_0 is the starting notch length and Y is a function for geometrical correction. It was shown and verified by model calculations, that the fracture resistance of different materials can be compared by this method.[36,37] The maximum value is interpreted as the formal fracture toughness, which is independent of different specimen dimensions and starting notch length. For a variety of different materials it was shown that the formal fracture toughness as well as the shape of the curve is significantly different.[37] Thus, a quantitative evaluation of the fracture resistance is possible. As the formal fracture toughness refers to the starting notch length it gives a lower bound of the effective fracture toughness which is based on the actual crack length.

4. Results and discussion

4.1. Mechanical properties at room temperature

The stiffness of the material was determined for the different matrix compositions, fibre volume contents and different

Table 2
Young's modulus and bending strength of unidirectional and bidirectional reinforced material with different matrix compositions, set in ratio to the fibre volume contents for comparability

Matrix composition	C-excess	Stoichiometric		Si-excess
Reinforcement	Unidirectional	Unidirectional	Bidirectional (0/90°)	Unidirectional
Young's-modulus E [GPa]	125 ± 13	110 ± 4	42 ± 9	95 ± 10
Fiber volume content V_f [−]	0.57	0.48	0.39	0.42
Ratio E/V_f [GPa]	219	229	108	226
Bending strength σ [MPa]	510 ± 40	360 ± 45	160 ± 15	230 ± 20
Fiber volume content V_f [−]	0.57	0.48	0.35	0.42
Ratio σ/V_f [MPa]	895	750	457	548

types of reinforcement. The fibre volume content decreased with increasing ratio of silicon within the matrix. Thus, in Table 2 for comparison the stiffness is presented as the ratio of Young's modulus and fibre volume content. It is obvious that there is no significant difference between these ratios for the different compositions. The Young's modulus measured for unidirectional reinforced material of 110 GPa is close to the product of fibre volume content and Young's modulus of the fibres (0.48 GPa × 238 GPa = 114 GPa). Furthermore, the result for 0/90°-laminates is close to half of the value for unidirectional reinforcement. All these results indicate that the stiffness is dominated by the layers with fibres oriented in the loading direction.

Regarding the rule of mixture for the stiffness of a composite it is evident that the stiffness of the porous matrix material is much lower than the stiffness of the fibres. This result leads to the conclusion that the developed material exhibits a fibre-dominated behaviour with the consequences as discussed in the introduction.

Since the bending strength of a fibre-dominated material is also determined by the fibres, the measured values are also presented as a ratio to the fibre volume content (Table 2). In contrast to the stiffness, the bending strength shows a dependency on the matrix composition: It decreases with increasing amount of silicon from a matrix with C-excess to a matrix with Si-excess.

In order to investigate the fracture behaviour SENB-tests were performed on 0/90°-laminates with different matrix compositions as described in Section 3. Representative results are plotted in Fig. 9. The slope of the curves and therefore the displacements are given by the Young's modulus and therefore by the fibre volume contents (49, 47 and 40%, respectively).

The material with an excess of carbon within the matrix shows a sharp load decrease. The curve is also almost linear up to maximum load – both observations indicate a brittle failure behaviour. Composites with a stoichiometric matrix material show a similar behaviour, but a slight deviation from linearity and the load decrease is slower. The material with an excess of silicon within the matrix shows, in contrast, an early deviation from linearity and a uniform decrease indicating a damage tolerant fracture behaviour and an uncorrelated fibre fracture.

The conclusions are confirmed by the analysis of the fracture surfaces (Fig. 10). The longitudinal and transverse arranged fibre layers are easily identified. Fig. 10(a) shows the fracture surface of a laminate with carbon excess within the matrix. The fracture surfaces of fibre bundles transverse to the crack direction are flat, the fibres and matrix are broken in one plane. There are no single fibres sticking out of the surface. This shows that the growing crack was not bridged by fibres but expanded in a brittle manner. As expected from the load-displacement-curves the fracture surface of material with stoichiometric matrix composition is slightly more jagged (Fig. 10(b)). Even some single fibres are observable at the bottom of the picture. The fracture behaviour is marginally more tolerant.

A different effect is visible in Fig. 10(c). The fibres stick out brush-like in the transverse layers. Such a fracture surface has also been described for oxide/oxide composites with porous matrices.[24] The expanding crack is initially bridged by the fibres before their strength is exceeded and they break, each one individual in an uncorrelated manner. Thus, it can be concluded that the strengthening effect of the fibres is utilised.

Taking into account this obviously improved crack bridging effects in the material with silicon excess it seems

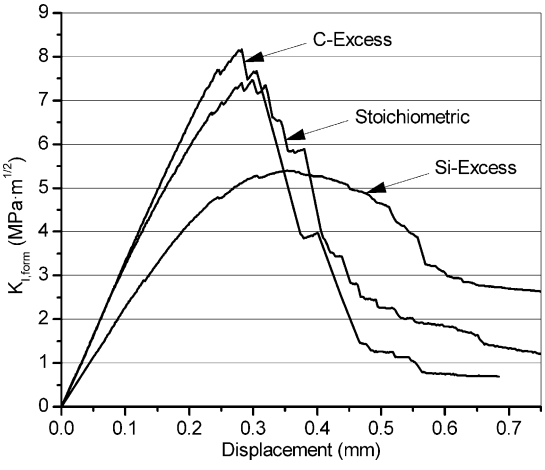

Fig. 9. Plot of formal stress intensity factor versus displacement for 0/90°-laminates with different matrix compositions.

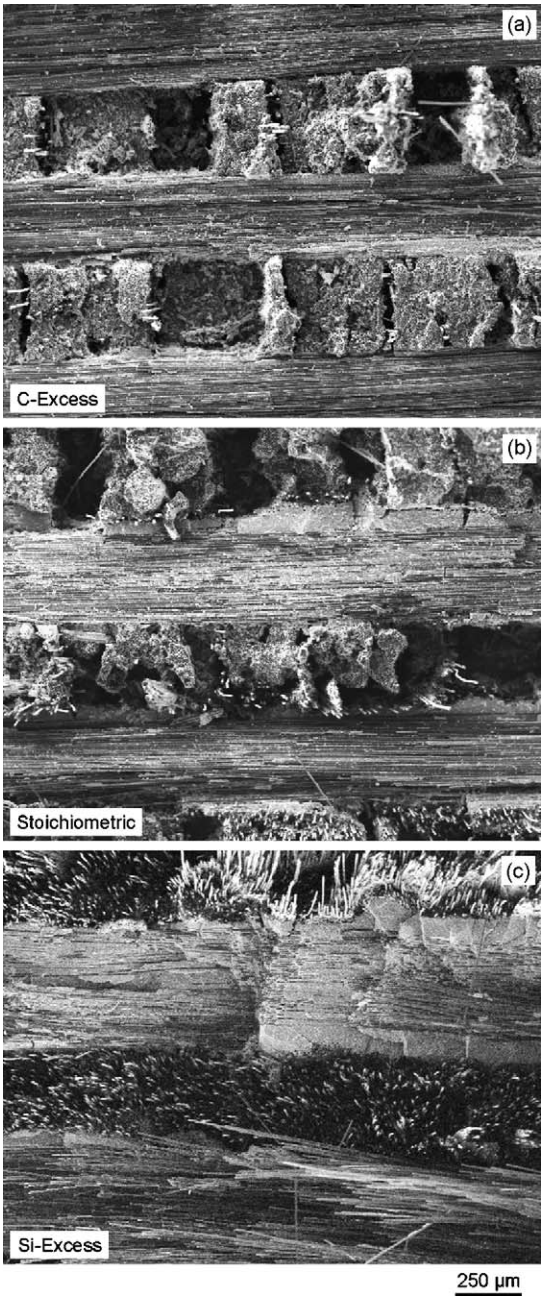

Fig. 10. SEM-micrographs of fracture surfaces after SENB-test; 0/90°-laminates with (a) matrix with C-excess, (b) stoichiometric matrix and (c) matrix with Si-excess.

surprisingly that it shows a significantly lower formal fracture toughness (Fig. 9) as well as bending strength (Table 2) than the material with lower silicon content. The fracture behaviour leads to the conclusion that the fibre strength is utilised and the strength of the composites reaches its capacity. An explanation is found in the XRD-measurements. Even though an excess of silicon is implemented in the precursor, no free silicon could be detected after the final reaction. It was shown that a fraction of the silicon is vaporised during silicon-carbon reaction. Silicon vapour may also react with the carbon fibres, thus degrading the fibre strength and leading therefore to a reduced composite strength. In contrast to the reaction within the matrix (liquid silicon reacts with solid carbon) more complicated gas phase reactions with the participation of silicon oxide are probable. The total porosity as well as the average pore radius is increased (see Section 2.2.1). These effects of silicon vaporisation and reaction of silicon with the carbon fibres are also assumed to be present in the material with lower silicon contents but to a lesser degree.

Table 3
Bending strength of unidirectional reinforced C/SiC with stoichiometric matrix composition, high temperature testing device

Testing temperature (°C)	Bending strength (MPa)
24	370 ± 35
1000	465 ± 40
1500	480 ± 20

In the case of the theoretical stoichiometric matrix composition an excess of glassy carbon is also expected (see also Section 2 and Fig. 2). The high adhesion between glassy carbon and the carbon fibres as shown in Fig. 4 leads to a more brittle fracture behaviour. A crack formed within the residual glassy carbon cannot be stopped at or deflected around the fibres. A flat fracture surface is formed and a sharp load decrease takes place, which causes brittle damage behaviour. This is clearly shown in the case of material with carbon excess within the matrix. In the case of a stoichiometric matrix composition the smaller amount of residual glassy carbon within the matrix is still sufficient to lead to a similar fracture behaviour, but the more jagged fracture surface as well as some protruding single fibres show, that only a slightly higher amount of silicon would suffice to avoid the carbon excess and to reach a completely non-brittle fracture behaviour as in the case of the material with the relatively high silicon excess within the matrix. Thus, by optimising the silicon excess, the amount of silicon that reacts with the carbon fibres could probably be reduced without loss of non-brittle behaviour but retaining a higher composite strength and fracture resistance.

4.2. High temperature bending strength

The bending strength of the unidirectional reinforced composites was measured in inert atmosphere at room temperature, 1000 °C and 1500 °C (i.e. above the temperature of the silicon-carbon reaction). The results show a promising tendency for high-temperature applications: There is an increase of the bending strength of 25 % up to 1500 °C (Table 3). This is mainly attributed to an increase of carbon fibre strength with increasing temperature. Furthermore, residual stresses are reduced when the test temperature is close to the manufacturing temperature.

Fig. 11(a) shows a representative stress-strain-curve from a three-point-bending test at room temperature of a unidirectional reinforced specimen with stoichiometric matrix composition. An almost linear stress-strain-behaviour up to fracture is typical for fibre-dominated materials. Due to the

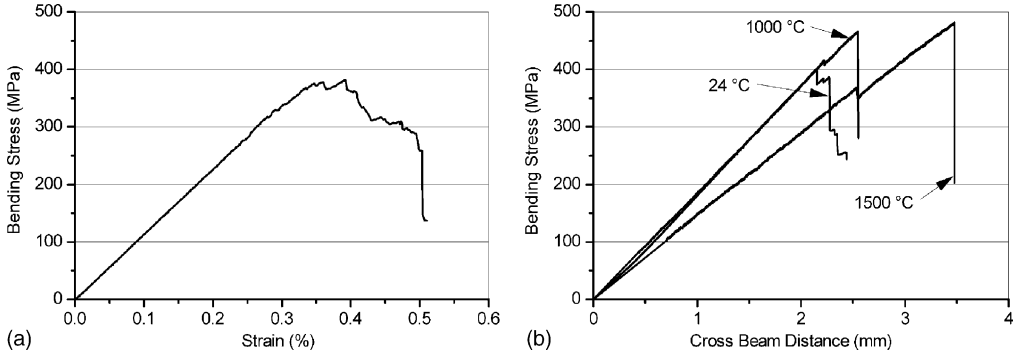

Fig. 11. Three-point-bending of unidirectional reinforced silicon carbide; (a) stress-strain-diagram at room temperature and (b) stress-displacement-diagram at different temperatures (high temperature testing device).

low stiffness of the matrix material, the stiffness of such composites is almost constant up to fracture even if matrix cracks develop. Thus, the fibres carry the main part of the load. Due to negligible stress redistribution between fibres and matrix and a high amount of stored energy the fracture behaviour of fibre-dominated material is usually brittle. In contrast, a gradual load decrease takes place in the case of the material developed here, which can be attributed to the sequential failure processes of the fibres.

A similar result at room temperature was found in the high temperature testing equipment (Fig. 11(b)). The specimens for measurements in this device were each of the same dimensions. Thus, the displacements at the different temperatures are comparable. At high temperatures (1000 and 1500 °C), the material shows a sharper load decrease than at room temperature due to the higher stress level and therefore a higher amount of stored energy.

At a temperature of 1500 °C the material shows a significantly lower stiffness than at temperatures below 1000 °C (Fig. 11(b)). This effect is attributed to a certain amount of oxygen within the material (analysed by EDAX), which is supposed to exist as SiO_2. This glass phase softens at a temperature of 1500 °C, so that even a small amount leads to a reduction of the overall stiffness.

4.3. Comparison to related materials

The strength reached by the 0/90°-laminate with stoichiometric composition in this work is comparable to that of a C/C-SiC-material produced by liquid silicon infiltration,[38] even though the present material had a significantly lower fibre volume content (35% instead of 65%). Moreover, the matrix in the material of this work was totally converted into silicon carbide. At high temperatures (up to 1500 °C) the strength of the C/SiC-material developed in this work was even higher. The bending strength (160 MPa) at room temperature is also close to a comparable standard C/C-material (CF 222) of Schunk Kohlenstofftechnik, Germany (200 MPa), which consists again of a high volume content of fibres (60%) and which is treated at a graphitisation-temperature of more than 2000 °C (versus 1450 °C using the in-situ silicon-carbon reaction).[39] The strength and fracture toughness are as expected significantly lower than that of high-quality, expensive C/SiC-materials with stiff matrices and fibre coatings for aerospace applications (bending strength up to 600 MPa, formal fracture toughness of more than 20 MPa × $m^{1/2}$ for bidirectional reinforced material).[40] All these related materials are reinforced with carbon fabrics, whereas the composite in this work is laminated. Nevertheless, as fibre type, matrix chemistry and/or porosity are similar, the comparison gives a reasonable impression of the competitive capability of the new material.

Due to an almost linear stress-strain-behaviour up to maximum load, the strain to failure results from the measured bending strength and the Young's modulus. The value of 0.34% for the unidirectional reinforced material (bidirectional reinforced: 0.51%) is significantly higher than that of monolithic silicon carbide material (0.15%).[7] The formal fracture toughness of the 0/90°-laminates (8 MPa × $m^{1/2}$) is more than twice as high as the fracture toughness of monolithic silicon carbide (2–4 MPa × $m^{1/2}$).[7] Both indicate the effect of reinforcement, even though it is typical that the bending strength of the composite is not as high as that of silicon carbide (up to 700 MPa for HIP-SiC).[7] The aim of the fibre reinforcement is to increase the fracture toughness as well as to provide a tolerant fracture behaviour.

The interlaminar shear strength (10 ± 2 MPa for unidirectional reinforced material) is relatively low, which is caused by the high level of matrix porosity. This is a general feature of fibre-dominated ceramic matrix composites. Carbon-fibre-reinforced carbon is also to be included among these materials, due to the low stiffness of the matrix carbon. Comparable material (CF 222) of Schunk Kohlenstofftechnik GmbH, Germany, has a specified interlaminar shear strength of 8 MPa, whereas high-quality C/SiC-material attains values of up to 48 MPa.[39,40]

The low linear coefficient of thermal expansion (CTE) in the temperature range from 200–1200 °C of 0–2 × 10^{-6} K^{-1} in the fibre direction is attributed to the fibre properties. The

CTE of carbon fibres in this temperature range is quoted as -0.5–$1 \times 10^{-6}\,K^{-1}$ in the axial direction.[2,41] The significantly higher value of silicon carbide ($4.5 \times 10^{-6}\,K^{-1}$) has only little influence, because of the dominating fibre stiffness. Transverse to the fibre direction, a thermal expansion in the temperature range of 200–1200 °C of 6–$7 \times 10^{-6}\,K^{-1}$ is expected from a simple rule of mixtures, which is applicable as a first approach for this orientation. The transverse CTE of the fibres is given by Savage as 10–$15 \times 10^{-6}\,K^{-1}$.[2]

5. Conclusions

A novel processing route to produce carbon-fibre-reinforced silicon carbide with a porous matrix material has been developed and characterised with regard to mechanical properties. The matrix is composed initially of silicon and carbon and a subsequent reaction forms silicon carbide. The investigations lead to the following conclusions:

1. The in-situ silicon-carbon reaction leads to a porous C/SiC-material with minimised fibre attack at a low cost comparable with the liquid silicon infiltration route.
2. The determination of the Young's modulus of material with different matrix compositions indicates that a fibre-dominated material is obtained. Bending strength as well as formal fracture toughness decreased with increasing content of silicon, which indicates a certain attack by silicon (gaseous reactants) and therefore a degradation of the fibres. Using the SENB-test, it could be shown that the damage tolerance of the material increases with increasing content of silicon within the matrix (increasing porosity).
3. The bending strength of the developed C/SiC-material increased by 25% up to 1500 °C, which indicates a potential for high temperature applications.
4. The mechanical properties (especially bending strength) are similar to C/C-SiC as well as C/C, which both also have to be considered as fibre-dominated materials. It is remarkable that this is realised with a significantly lower fibre volume content in this new material.
5. The possibility of forming a porous matrix to obtain a fibre-dominated material has been demonstrated for a non-oxide material. It has been found that the reduction of stress concentrations due to effects of the matrix could be utilised at relatively low levels of fibre volume content (35% up to a maximum of 50%). The distribution of fibres and matrix should be as homogeneous as possible with a sufficient matrix surrounding each fibre.
6. Furthermore, in contrast to previous evaluations a gradual load decrease and therefore a pseudo-plastic fracture behaviour was found in the load-displacement-curves of bending tests at room temperature.
7. In order to avoid segmentation cracks observed in bi-directional laminates a multi-directional material might be easily realised by conventional winding techniques.

References

1. Bunsell, A. R., Ceramic fibres for reinforcement. In *Ceramic-Matrix Composites*, ed. R. Warren. Chapman and Hall, New York, 1992, pp. 12–34.
2. Savage, G., *Carbon-Carbon Composites*. Chapman and Hall, London, 1993.
3. Lange, F. F., Levi, C. G. and Zok, F. W., Processing fiber reinforced ceramics with porous matrices. In *Carbon/Carbon, Cement, and Ceramic Matrix Composites*, ed. R. Warren. In *Comprehensive Composite Materials*, *vol.4*, ed. A. Kelly and C. Zweben. Amsterdam, Elsevier, 2000, pp. 427–448.
4. Evans, A. G. and Zok, F. W., Review: The physics and mechanics of fibre-reinforced brittle matrix composites. *J. Mater. Sci.*, 1994, **29**, 3857–3869.
5. Evans, A. G. and Marshall, D. B., Overview No. 85. The mechanical behavior of ceramic matrix composites. *Acta Metall.*, 1998, **37**, 2567–2583.
6. Grathwohl, G., Kuntz, M., Pippel, E. and Wolterdorf, J., The real structure of the interlayer between fibre and matrix and its influence on the properties of ceramic composites. *Physica Status Solidi (a)*, 1994, **146**, 393–414.
7. Chawla, K. K., *Ceramic Matrix Composites*. Chapman and Hall, London, 1993.
8. Fitzer, E. and Gadow, R., Fiber-reinforced silicon carbide. *Am. Ceram. Soc. Bull.*, 1986, **65**, 326–335.
9. Strife, J. R., Brennan, J. J. and Prewo, K. M., Status of continuous fiber-reinforced ceramic matrix composite processing technology. *Ceram. Eng. Sci. Proc.*, 1990, **11**, 871–919.
10. Huettinger, K. J. and Greil, P., Ceramic composites for applications at extremely high temperatures. *cfi/Ber DKG*, 1992, **69**, 445–460.
11. Langlais, F., Chemical vapor infiltration processing of ceramic matrix composites. In *Carbon/Carbon, Cement, and Ceramic Matrix composites*, ed. R. Warren. In *Comprehensive Composite Materials*, *vol.4*, ed. A. Kelly and C. Zweben. Amsterdam, Elsevier, 2000, pp. 611–644.
12. Naslain, R. and Langlais, F., CVD-processing of ceramic-ceramic composite materials. *Mater. Sci. Res.*, 1986, **20**, 145–164.
13. Naslain, R., CVI composites. In *Ceramic-Matrix Composites*, ed. R. Warren. Chapman and Hall, New York, 1992, pp. 199–244.
14. Mühlratzer, A., Design of gradient-CVI derived CMC components. *Indus. Ceram.*, 1996, **16**, 111–117.
15. Suttor, D., Erny, T., Greil, P., Goedecke, H. and Haug, T., Fiber-reinforced ceramic-matrix composites with a polysiloxane/boron-derived matrix. *J. Am. Ceram. Soc.*, 1997, **80**, 1831–1840.
16. Zheng, G. B., Sano, H., Uchiyama, Y., Kobayashi, K. and Cheng, H. M., The properties of carbon fibre/SiC composites fabricated through impregnation and pyrolysis of polycarbosilane. *J. Mater. Sci.*, 1999, **34**, 827–834.
17. Ziegler, G., Richter, I. and Suttor, D., Fiber-reinforced composites with polymer-derived matrix: processing, matrix formation and properties. *Composites: Part A*, 1999, **30**, 411–417.
18. Ly, H. Q., Taylor, R. and Day, R. J., Carbon fibre-reinforced CMCs by PCS infiltration. *J. Mater. Sci.*, 2001, **36**, 4027–4035.
19. He, M. Y. and Hutchinson, J. W., Crack deflection at an interface between dissimilar elastic materials. *Int. J. Solids Struct.*, 1998, **25**, 1053–1067.
20. Luthra, K. L., Singh, R. N. and Brun, M. K., Toughened silcomp composites – process and preliminary properties. *Am. Ceram. Soc. Bull.*, 1993, **72**, 79–85.
21. Krenkel, W., Cost effective processing of CMC composites by melt infiltration (LSI-process). In 25th Annual International Conference on Advanced Ceramics & Composites 2001, Cocoa Beach (Florida, USA), American Ceramic Society, January 2001.
22. Weiss, R., Carbon fibre reinforced CMCs: manufacture, properties, oxidation protection. In *High Temperature Ceramic Matrix*

composites, ed. W. Krenkel, R. Naslain and H. Schneider. Wiley-VCH, Weinheim, 2001, pp. 440–456.
23. Schulte-Fischedick, J., Zern, A., Mayer, J., Rühle, M., Frieß, M., Krenkel, W. and Kochendörfer, R., The morphology of silicon carbide in C/C-SiC composites. *Mater. Sci. Eng. A*, 2002, **332**, 146–152.
24. Zawada, L. P., Longitudinal and transthickness tensile behavior of several oxide/oxide composites. *Ceram. Eng. Sci. Proc.*, 1998, **19**, 327–340.
25. Kramb, V. A., John, R. and Zawada, L. P., Notched fracture behavior of an oxide/oxide ceramic-matrix composite. *J. Am. Ceram. Soc.*, 1999, **82**, 3087–3096.
26. Levi, C. G., Yang, J. Y., Dalgleish, B. J., Zok, F. W. and Evans, A. G., Processing and performance of an all-oxide ceramic composite. *J. Am. Ceram. Soc.*, 1998, **81**, 2077–2086.
27. Lange, F. F., Tu, W. C. and Evans, A. G., Processing of damage-tolerant, oxidation-resistant ceramic matrix composites by a precursor infiltration and pyrolysis method. *Mater. Sci. Eng. A*, 1995, **195**, 145–150.
28. Tu, W. C., Lange, F. F. and Evans, A. G., Concept for a damage-tolerant ceramic composite with "strong" interfaces. *J. Am. Ceramic Soc.*, 1996, **79**, 417–424.
29. Lange, F. F., Radsick, T. C. and Holmquist, M., Oxide/oxide composites: control of microstructure and properties. In *High Temperature Ceramic Matrix Composites*, ed. W. Krenkel, R. Naslain and H. Schneider. Wiley-VCH, Weinheim, 2001, pp. 587–599.
30. Kanka, B. and Schneider, H., Aluminosilicate fiber/mullite matrix composites with favorable high-temperature properties. *J. Europ. Ceram. Soc.*, 2000, **20**, 619–623.
31. Kanka, B. J., Schmücker, M., Luxem, W. and Schneider, H., Processing and microstructure of WHIPOX™. In *High Temperature Ceramic Matrix Composites*, ed. W. Krenkel, R. Naslain and H. Schneider. Wiley-VCH, Weinheim, 2001, pp. 610–615.
32. Heathcote, J. A., Gong, X. Y., Yang, J. Y., Ramamurty, U. and Zok, F. W., In-plane mechanical properties of an all-oxide ceramic composite. *J. Am. Ceram. Soc.*, 1999, **82**, 2721–2730.
33. Mattoni, M. A., Yang, J. Y., Levi, C. G. and Zok, F. W., Effects of matrix porosity on the mechanical properties of a porous-matrix, all-oxide ceramic composite. *J. Am. Ceram. Soc.*, 2001, **84**, 2594–2602.
34. She, J., Mechnich, P., Schneider, H., Schmuecker, M. and Kanka, B., Effect of cyclic infiltrations on microstructure and mechanical behavior of porous mullite/mullite composites. *Mater. Sci. Eng. A*, 2002, **325**, 19–24.
35. *EN 658-5: Advanced Technical Ceramics; Mechanical properties of ceramic composites at room temperature. Part 5: Determination of shear strength by short span bend test (Three-point)*. German version. European Committee for Standardisation, 2002.
36. Rausch, G., Kuntz, M. and Grathwohl, G., Determination of the in situ fiber strength of ceramic-matrix composites from crack-resistance evaluation using single-edge notched-beam tests. *J. Am. Ceram. Soc.*, 2000, **83**, 2762–2768.
37. Kuntz, M., *Risswiderstand keramischer Faserverbundwerkstoffe*. Ph.D. thesis, University of Karlsruhe, Karlsruhe, Germany, 1995.
38. Krenkel, W., Heidenreich, B. and Renz, R., C/C-SiC composites for advanced friction systems. *Adv. Eng. Mater.*, 2002, **4**, 427–436.
39. Schunk Kohlenstofftechnik GmbH, Werkstoff CF 222. Datenblatt. Data Sheet. Heuchelheim, August 2003.
40. Muehlratzer, A. and Leuchs, M., Applications of non-oxide CMCs. In *High Temperature Ceramic Matrix Composites*, ed. W. Krenkel, R. Naslain and H. Schneider. Wiley-VCH, Weinheim, 2001, pp. 288–298.
41. Sauder, C., Lamon, J. and Pailler, R., Thermomechanical properties of carbon fibres at high temperatures (up to 2000 °C). *Compos. Sci. Technol.*, 2002, **62**, 499–504.